19

Virtual Crack Closure Technique and Finite Element Method for Predicting the Delamination Growth Initiation in Composite Structures

Pietropaoli Elisa
Cira, Italian aerospace research center
Italy

1. Introduction

Even thought composite materials have been introduced in aircraft industries since the middle of the last century, only the quite recent decision of the most important aircraft suppliers to use extendedly these advanced materials for their new aircrafts (AIRBUS-A380 and BOEING-787) have made people aware on the great potentiality of composites in strategic fields. It is not rare to see in newspapers composite materials to be referred as "plastics", really, if composites were only "plastics" they would not be used for such strategic applications. Indeed, composite materials for aerospace structures are properly "Fiber Reinforced Plastics" being the great advantages associated to the use of composites brought by the combination on a macroscopic scale of two constituents, namely reinforcing fibers and matrix (polymeric for example).
Thus, the principal difference between composites and other materials obtained by combining more elements (such as metals alloys) lies in the fact that composite materials constituents differ at molecular level to each other and are mechanically separable (Jones R,1999)-(Mazumdar,2002).
It is well known that the same material has higher stiffness and strength in the fiber form than in the bulk one because of the reduced number of defects, such as dislocations, that it contains. Being a single fiber of microscopic diameter useless to realize any load-carrying structure, the basic idea is to join and keep fibers in the required positions by embedding them into a matrix (polymeric, metal, ceramic) in order to obtain a material whose properties could be improved with respect to the ones of the constituents.
Thus, within a composite material fibers are the load-carrying elements which provide the required stiffness and strength while the matrix material binds the fibers together and transfers the load between them.
Since composites are materials that "can be built", they can be designed to fulfil requested requirements in terms of both mechanical properties and corrosion and electrical behaviour.
Many advantages can be obtained by using composites instead of traditional engineering materials (such as improved specific stiffness and strength), however high costs and lacks of knowledge in their behaviour do not make the use of composite materials easy at all.
In terms of engineering analysis of the mechanical behaviour of composites the major concern is about their inherently anisotropy. For example, the application of a load in a

direction that is not principal for the material leads to coupling effects between shear and extension thus the application of a normal stress induces not only an extension in the direction of the stress and a contraction perpendicular to it but also a shearing deformation (Jones R,1999).
A lot of composite material types have been developed (i.e with short or long reinforcing fibres), however in the following only composites made of long and continuous fibers embedded in a polymeric matrix are addressed.
Furthermore, only macromechanics aspects of these materials are accounted for, thus assuming the material homogeneous and the effects of the constituents detected only as an averaged macroscopic properties of the composites.
As above said composites can be tailored to achieve specific requirements, for example in terms of strength and stiffness of the material itself. However, in terms of design of structures different laminae or ply with different fibers orientation of composites materials can be stacked and bonded together in order to obtain a laminate composite material whose properties meet definite design needs in particular directions without wasting of materials where stiffness and strength are not required.
Due to the inherent anisotropy of the material, the damage phenomenology of composite laminate is quite complex (Altenbach et al., 2004). Failure strongly depends on the stress distribution within the material which is surely associated to the intensity of the applied load but also on its direction and on the laminate stacking sequence.
Literature classified fracture modes (Pagano & Schoeppner, 2003) of composite laminates in:

- Intralaminar failure: fracture is located inside the lamina (i.e matrix crack, fiber breakage, matrix-fiber debonding, fiber kinking)
- Interlaminar failure: fracture occurs between two adjacent plies and lies in a plane parallel to that of the fibers (i.e delamination)
- Translaminar failure: fracture is oriented transverse to the laminate plate

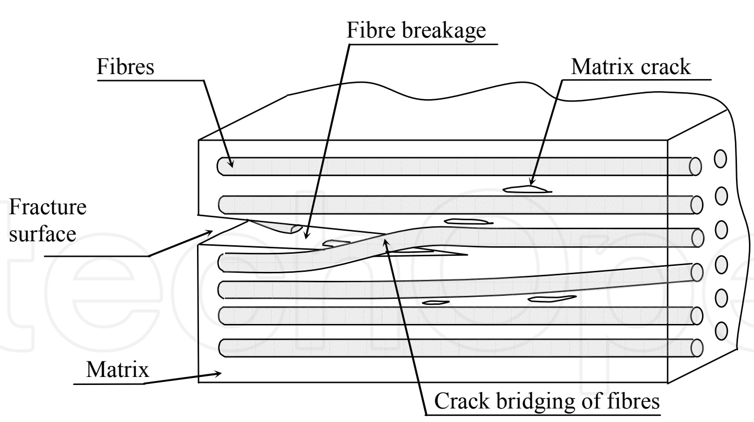

Fig. 1. Failure modes of unidirectional composites

A simplified sketch of failure modes in unidirectional composites was proposed by Pagano & Schoeppner (2003) as shown in Figure 1.

2. Interlaminar damage: Delaminations

Delaminations are probably the most critical and studied, failure mode of composite material. In the composites literature, delamination is generally assumed to take place at the interface between adjacent plies and treated as a fracture process between anisotropic layers, rather than to consider it, more precisely, as a fracture between constituents or within one of the constituents (such as the material matrix) (Pagano & Pipes, 1971).

Delamination can onset due to manufacturing (drilling, residual thermal stress induced by the cure process) or to low velocity impact of dropping tools or runway debris. Furthermore delamination may be induced by interlaminar shear and normal stresses associated to some geometrical configurations such as free edges, curved sections as well as tapers and transitions. Whichever their cause is, delaminations may buckling and growth under service conditions thus leading to the premature collapse of the structure as well as to the premature buckling of the laminate, intrusion of moisture, stiffness degradation, and loss of fatigue life.

The through-thickness weakness of composite laminates results in poor response to impact damage. Impacts are generally classified based on impactor velocity or on their energy. Low velocity impacts are typically impacts in which a large object falls onto the structure with low velocity while high velocity impacts are impacts resulting in complete perforation of the target (Abrate, 1998).

A low velocity impact event usually results in a combination of failure modes including matrix crack, local fiber breaking at the front-face impacted surface, back-face ply splitting and fiber breaks, and multilevel delamination (Pagano & Schoeppner, 2003). All these damage cannot be detected during visual inspection therefore are defined Barely Visible Impact Damage (BVID) but they may reduce consistently the strength of the structure.

The amount of damage induced in the structure depends, also in this case, the laminate stacking sequence. It has been observed that delaminations occur only at interfaces between plies with different fiber orientation (Abrate, 1998) and in general are introduced at several interfaces within the same laminate. Furthermore, it has been found that the delaminated area has an oblong of "peanut shape" whose major axis is oriented in the direction of the fiber of the lower ply of the delaminated interface away from the impact surface.

Experimental non-destructive technique such as C-Scan and X-Ray provide a projection of these entire damaged surface on a single plane.

Thus, by overlaying the plan view of each of the individual interface delaminations, the resultant damaged area may appear to be a nearly circular or an elliptical continuous region.

The damage pattern is strongly influenced by the thickness of the impacted laminate that determines the laminate bending stiffness or the duration of the contact between the laminate and the impactor. Thin laminate subjected to impact tends to bend consistently, this results in large in-plane tensile stresses that exceed the transverse tensile strength of the plies near the back face of the laminate leading to matrix cracking and delamination (damage progress from the bottom therefore the damage pattern is referred as reversed pine tree as shown in Figure 2, a).

Thick laminates behave a low bending compliance that results in significant transverse normal and shear contact stress leading to matrix cracking in the contact region and delamination between the plies near the impacted surface (Pagano & Schoeppner, 2003 and Abrate,1998), pine tree damage pattern shown in Figure 2, b.

Two different considerations are generally used for the design of composite structures namely damage resistance and damage tolerance. The damage resistance can be defined as the measure of the capability of a material or structure to resist the initial occurrence of damage (Pagano & Pipes, 1971). Whereas, the damage tolerance is a measure of a damaged material or damaged structure to sustain load and/or maintain functional capability.

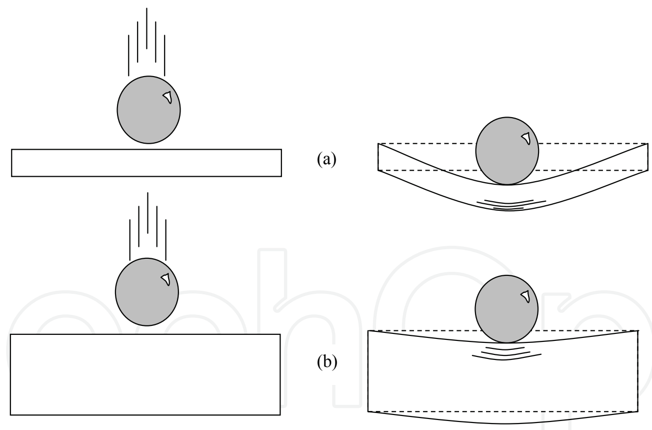

Fig. 2. Impact on thin (a) and thick (b) laminates

The damage resistance may be quantified by measuring the load at which damage initiates during a single impact event on an undamaged specimen. In literature a huge amount of works have been devoted to the analysis of the damage resistance determination in case of low velocity impact on composite laminates.

Worth of noting are, amongst the others, the works by Davies and Zhang (Davies & Zhang, 1995)-(Davies et al., 1994) devoted to the development of a theoretical method for the prediction of the threshold fracture load in low velocity impacts as well as the determination of the extent of the damaged area.

In order to improve the damage resistance of composite structure to the delamination onset, the design should be aimed at minimizing interlaminar stresses by avoiding critical shapes (curved sections, ply drop off and so on) and selecting opportunely the laminate stacking sequence.

Damage tolerance considerations are generally based on experimental investigations. The stiffness and strength reduction associated to the presence of a delamination in composite laminate plates is very strong especially in compression. A common measure of the damage tolerance of impacted laminates is obtained by performing compression after impact (CAI) tests. Within these tests, a damaged structure, is progressively loaded until the structural collapse is reached and the design allowables are determined accounting for the presence of undetected delamination or intralaminar damage.

Nowadays there is a wide demand of numerical tools capable to measure the damage tolerance of aircraft composite structures and this explains why many research activities are dealing with the development of numerical methodologies with predictive capabilities.

In order to generate experimental data to be used for validating numerical models dealing with delamination, experimental tests (CAI) are generally performed by creating an artificial debonding between two adjacent layers of a composite laminate through the insertion of a very thin film of Teflon (Kyoung & Kim, 1995).

Two edges of the structure are then clamped in a test machine and a compressive displacement is gradually applied. The composite laminate is subdivided by the delamination into a thin sub-laminate and a thick sublaminate or base sublaminate. Different kinds of configuration (local and global instabilities) may appear at different load levels and they can be monitored by following the out of plane displacement of two control points (U and L in Figure 3) placed on the two sub-laminates.The behaviour commonly observed during these tests can be described as follows (Riccio & Pietropaoli,2008). As the load increases the thin sublaminate buckles first. Afterwards, the buckling of the base sublaminate is induced. In this case, depending on the thicknesses ratio of the two sub-laminates, the out of plane displacement of the base sublaminate can be of the same sign (Type I) or of different sign (Type II) with respect to the one of the thin sub-laminate. When the buckling is of Type II, an increase in applied load determines the condition known as global buckling: the thin sublaminate is dragged towards the base sublaminate but the delamination opening continues to be relevant.

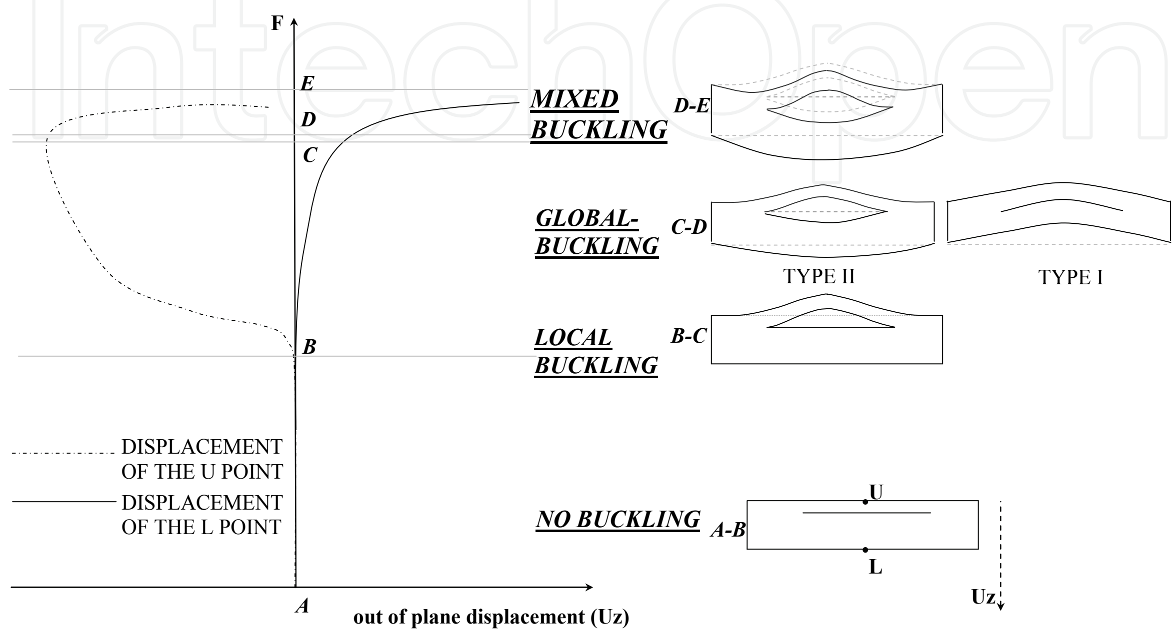

Fig. 3. Buckling configurations

3. Virtual crack closure technique

A delamination can be assimilated to a fracture process between anisotropic layers (interlaminar damage). Thus, fracture mechanics principles (Janssen et al., 2004) can be used to study the behaviour of composite structures in presence of interlaminar damage and to determine the conditions for the delamination growth initiation.
Under the assumption of considering the delamination growth process as a crack propagation phenomenon (Kachanov, 1988), fracture mechanics concepts can be generally transferred to the analysis of delaminated composite structures.
The propagation of a crack is possible when the energy released for unit width and length of fracture surface (named Strain Energy Release Rate, G) is equal to a threshold level or fracture toughness, characteristic for each material (Janssen et al., 2004).
Starting from the earlier analytical works by Chai et al., (1981) and Kardomates (1987), delamination in composites has been studied by evaluating the Strain Energy Release Rate. Nowadays, the G calculation is generally performed by means of techniques used in conjunction with the finite element method, such as the Virtual Crack Closure Technique.
According to the Virtual Crack Closure Technique, the evaluation of the Strain Energy Release Rate can be obtained starting from the assumption that for an infinitesimal crack opening, the strain energy released is equal to the amount of the work required to close the crack. Therefore, the work *W* required to close the crack can be evaluated by performing two analyses. The first analysis is needed to evaluate the stress field at the crack tip for a crack of

length *a* and the second one is aimed to obtain displacements in the configuration with the crack front appropriately extended from a to $a+\Delta a$ (Figure 4). The expression of the work *W* evaluated according to the two-steps Virtual Crack Closure Technique is given by Eq. (1).

$$W = \frac{1}{2}\left(\int_0^{\Delta a} \sigma_{yy}^{(a)}(x)\delta u_y^{(b)}(x)dx + \int_0^{\Delta a} \sigma_{yx}^{(a)}(x)\delta u_x^{(b)}(x)dx + \int_0^{\Delta a} \sigma_{yz}^{(a)}(x)\delta u_z^{(b)}(x)dx \right) \tag{1}$$

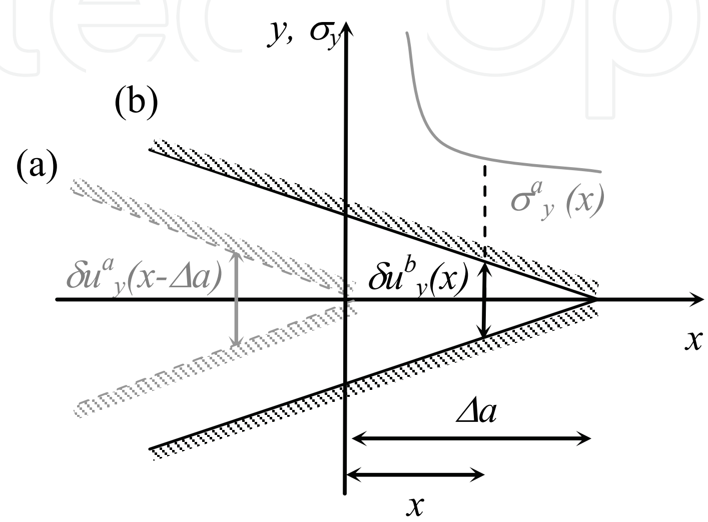

Fig. 4. Two-steps virtual crack closure technique: schematization of the two configurations before (a) and after the crack extension (b)

The quantities indicated in Eq. (1) with the apex (a) and (b) are evaluated in configuration (a) and (b) of Figure 4 respectively describing the crack tip status, before and after the crack propagation.

The calculation of the Strain Energy Release Rate can be simplified by adopting an alternative approach: the one step Virtual Crack Closure Technique (VCCT). The VCCT is based on the assumption that an infinitesimal crack extension has negligible effects on the crack front therefore both stress and displacement can be evaluated within the same configuration by performing only one analysis.

By adopting this technique, the expression of the work W required to close the crack becomes as in Eq. (2).

$$W = \frac{1}{2}\left(\int_0^{\Delta a} \sigma_{yy}^{(a)}(x)\delta u_y^{(a)}(x-\Delta a)dx + \int_0^{\Delta a} \sigma_{yx}^{(a)}(x)\delta u_x^{(a)}(x-\Delta a)dx + \int_0^{\Delta a} \sigma_{yz}^{(a)}(x)\delta u_z^{(a)}(x-\Delta a)dx \right) \tag{2}$$

where both displacements and stress are evaluated in the configuration (a) of Figure 4. According to the definition previously given, the Energy Release Rate can be written as in Eq.(3).

$$G = \lim_{\Delta a \to 0} \frac{W}{\Delta a} \tag{3}$$

Combining Eq.(2) and (3) it is possible to obtain the expression of the Strain Energy Release Rate for the three mutually orthogonal fracture modes: GI associated to the mode I or opening; GII to the mode II or in-plane shear, GIII to the mode III or antiplane shear. These three basic fracture modes are shown in Figure 5.

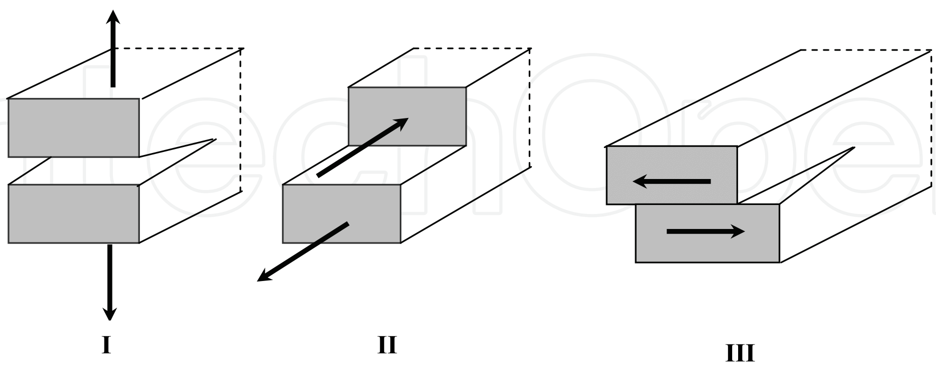

Fig. 5. VCCT schematization of the two configurations before (a) and after the crack extension (b)

3.1 Delamination growth criteria

In fracture mechanics, the Strain Energy Release Rate (G) is the quantity that, compared with the material fracture toughness (G_C), characterizes the state of the delamination (no growth, growth initiation, stable or unstable growth). As said before, G must be larger than Gc before crack growth occurs (Eq.4).

$$G > G_C \tag{4}$$

However, three different fracture modes can be defined associated to three orthogonal modes of loading (see Figure 5). For composites, it is extremely important to consider effect of the mode mixities on the delamination behaviour. Indeed, a delamination may be loaded in one of these modes or rather in some combination of these modes (Reeder, 2006).

Experimental tests are used to measure the critical fracture toughness but unfortunately, several different types of specimens are needed to generate delamination toughness data over a desired range of mixed-mode combinations (Reeder & Crews, 1990).

Results of these kinds of tests can be presented by plotting the mode I component of fracture toughness G_{IC} against the mode II component G_{IIC}.

Delamination growth criteria may be viewed as curve fit to fracture test data plotted in mixed mode diagrams. Thus, the accuracy of a failure criterion can be checked by seeking its capability to fit the material response when plotted on these diagrams.

Due to a late development of Mode III tests, most criteria available in literature, have been conceived taking into account only the first and the second interlaminar fracture modes. However, currently three dimensional criteria (Reeder, 2006) have been developed too.

One of the most used criterion is the power law Eq. (5) which may be used to represent a wide range of material responses by selecting opportunely the two exponents α, β.

$$\text{Power law criterion } \left(\frac{G_I^m}{G_{IC}}\right)^{\alpha} + \left(\frac{G_{II}^m}{G_{IIC}}\right)^{\beta} + \left(\frac{G_{III}^m}{G_{IIIC}}\right)^{\chi} = 1 \tag{5}$$

Another one is the Benzeggagh & Kenane (1996) criterion or B-K criterion, which requires the selection of only one fitting parameter η (Eq. (6)).

$$\text{B-K criterion} \quad \frac{G_T}{G_{IC} + \left[\left(G_{IIC} - G_{IC} \right) \frac{G_{II}^m}{G_T} + \left(G_{IIIC} - G_{IC} \right) \frac{G_{III}^m}{G_T} \right] \left(\frac{G_{II}^m + G_{III}^m}{G_T} \right)^{\eta - 1}} = 1 \tag{6}$$

It is clear that the proposed criteria are only mathematical expressions able to represent different material responses by varying the values assigned to the fitting parameters. Thus, the selection of these parameters requires that mixed-mode testing be performed during the characterization of the material.

3.2 Finite element models for computing the strain energy release rates by using the VCCT

Analytic computations of stresses and displacement at the crack tip are possible only in a few simplified cases ((Janssen et al., 2004)-(Chai et al., 1981), whereas numerical solutions may be found quite easily by using the Finite Element Method also for complex geometry. Indeed, the VCCT is generally used for the evaluation of the Strain Energy Release Rate in finite element analyses.

The first VCCT approach to compute Strain Energy Release Rates, starting from forces at the crack tip and relative displacements of the crack faces behind it, was proposed for four noded elements by Rybicki & Kanninen (1977).

After it was extended to higher order elements by Raju (1987) and to three-dimensional cracked bodies by Shivakumar et al. (1988). A comprehensive review of VCCT formulae for different element types was given by Krueger (2004). Whitcomb (1989) was one of the first to introduce the use of the VCCT to determine Strain Energy Release rate distributions for a circular delamination.

Since then, a lot of numerical analyses have been performed by using this technique: many of them dealing with delamination growth initiation (Mukherjee et al., 1994)-(Whitcomb,1992), others with growth evolution (Klug et al., 1996)-(Shen et al., 2001)-(Xie & Biggers, 2006)-(Pietropaoli & Riccio A., 2010a and 2010b) and skin-stringer debonding (Orifici et al., 2008)-(Wang & Raju 1996)-(Krueger & O'Brien, 2000).

When dealing with three-dimensional problems, the one-step Virtual Crack Closure Technique (VCCT) is generally used instead of the two-steps Virtual Crack Closure Technique in order to reduce the computational time requested for the analysis.

In the last years a wide spreading interest has been focused on cohesive elements (Camanho et al., 2003)-(Turon et al., 2004), because, based on both the strength of material formulation for crack initiation and fracture mechanics for crack propagation, they are able to overcome one important limitation of the VCCT: the need to define an initial delamination.

However, cohesive elements still pose problems in the definition of the constitutive model for interlaminar damage to be used.

Therefore, even if more rough in some aspects, the VCCT still continue to attract the attention, due to the simplicity of its theory and to its suitability for implementations in post-processing subroutines.

A delamination is merely a debonding between two adjacent parts of the same structure along the thickness. This debonding can be simulated in the finite element method by maintaining not merged nodes on two adjacent faces of the volumes or surfaces representing respectively two sublaminates (Figure 6).

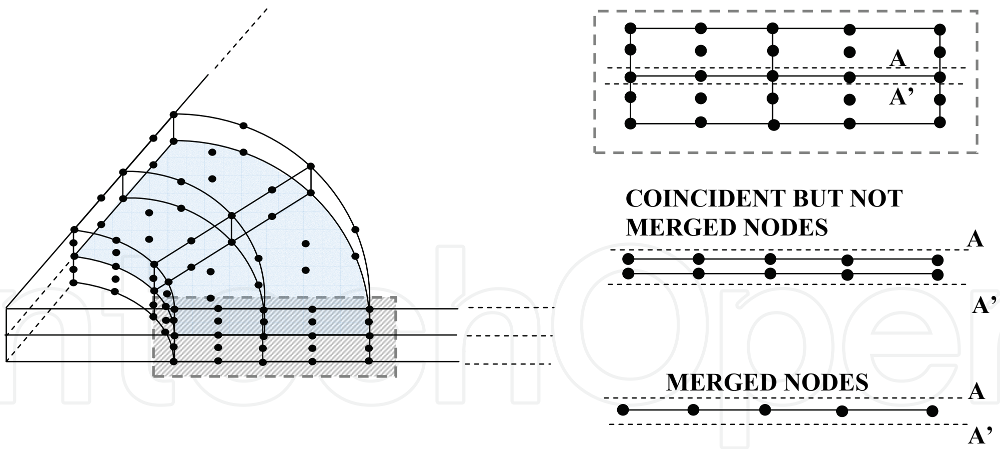

Fig. 6. A delamination can be simulated by maintaining not merged nodes with identical coordinates belonging to adjacent elements

Node pairs on adjacent interfaces can be connected by means of Multipoint constraints (Cook, 1995) or equivalently by relations between degree of freedom of these nodes. Indeed, node pairs in the debonded area are not connected but contact elements are introduced to avoid overlaps.
By proceeding in this way the evaluation of the Strain Energy Release Rate along the crack front, even if three-dimensional, can be obtained by using only nodal forces and displacements.
An example of application of the VCCT to a circular delamination is shown in Figure 7.

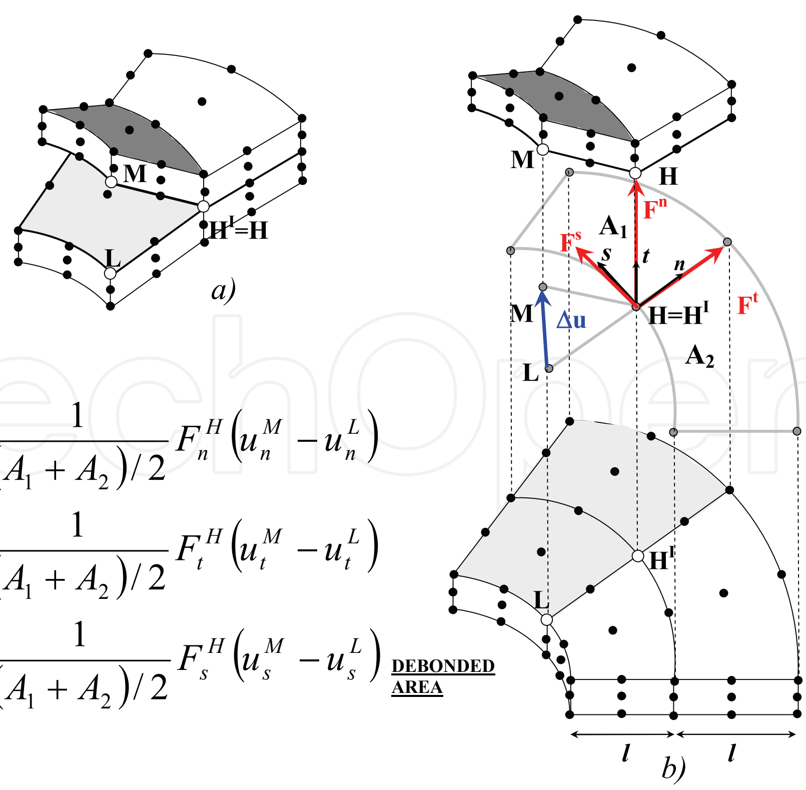

$$G_I^H = \frac{1}{2}\frac{1}{(A_1 + A_2)/2} F_n^H \left(u_n^M - u_n^L\right)$$

$$G_{II}^H = \frac{1}{2}\frac{1}{(A_1 + A_2)/2} F_t^H \left(u_t^M - u_t^L\right)$$

$$G_{III}^H = \frac{1}{2}\frac{1}{(A_1 + A_2)/2} F_s^H \left(u_s^M - u_s^L\right)$$

Fig. 7. Force at the crack tip (measure at the node H=H') and displacements (components of the vector connecting the nodes L and M)

The Eq. (7) can be used to compute Strain Energy Release rate components. It is worth noting that these components are referred to a local reference system (t,s,n).
The mesh in Figure 4 has been realised with elements of the same length (l) in the direction orthogonal to the delamination front.
Krueger (2004) has proposed corrections to VCCT formulae for elements with different lengths or widths at the crack tip.
Okada et al. (2005) proposed corrections for skewed and non-symmetric mesh arrangement at the crack front. The mesh of the finite element model can have edges parallel or orthogonal to the delamination front (as in Figure 6 and Figure 7), in this case it is called "orthogonal mesh", otherwise the mesh is "non orthogonal".
When orthogonal meshes are used, the delamination front can be easily individuated, otherwise algorithms for tracing the delamination front can be used (Xie & Biggers, 2006)-(Liu et al., 2011).

4. Application

The capabilities of the proposed approach to predict the delamination growth initiation has been verified on a test-case taken from literature (Sun et al., 2001).
The benchmark selected is a laminated composite plate characterized by the presence of an embedded elliptical delamination with semi axes of length 30 mm (in the applied load direction) and 15 mm (in the transverse direction).
Numerical data are available in literature (Sun et al., 2001) in terms of out of plane displacement versus load of two control points placed in the middle of the plate (respectively on the top of the thinnest sublaminate and on the bottom of the thickest or base sublaminate) and delamination growth initiation load. The specimen has a total length of 100 mm, it is clamped at four edges along the out of plane direction and a static compressive load is applied along the x-axis direction. The delamination is placed between the forth and the fifth ply over 32 plies. The laminate stacking sequence is $[(0°_2/90°_2]_{4S}$ with a nominal ply thickness of 0.127 mm. The material properties are reported in Table 1.

Longitudinal Young's Modulus	E_{11}	*134 GPa*
Transverse Young's Modulus	$E_{22} = E_{33}$	*10.2 GPa*
Shear Modulus	$G_{12} = G_{13}$	*5.52 GPa*
	G_{23}	*3.43 GPa*
Poisson's Ratio	$\nu_{12} = \nu_{13}$	*0.3*
	ν_{23}	*0.49*
Critical strain energy release rate for mode I	G_{IC}	*200 J/m²*
Critical strain energy release rate for mode II	G_{IIC}	*500 J/m²*

Table 1. Material properties

4.1 Analytical results

It is worth noting that for this geometrical configuration it is possible to obtain an analytical estimation of the critical values of the applied strain at which there are respectively the local buckling (ε_{CR}) and the delamination growth initiation (ε_{GR}). The analytical expressions proposed by Chai et al. (1981) are valid under the hypothesis that the material is isotropic, homogeneous and linear elastic. Even thought the benchmark selected is in composites, being the plies oriented at 0° and 90° and the laminate symmetric, the material behaviour can be assumed to be equivalent to that of an isotropic material. The equivalent Young's modulus E_{eq} can be obtained by using the formulae of the Classical Lamination Theory (CLT) in Jones (1999) and Kollar & Springer (2007). By using the CLT an equivalent Young's modulus for the composite material under consideration has been found to be equal to 72GPa. The data needed for the application of the analytical expressions proposed by Chai et al. (1981) are summarized in Table 2. Looking at the values in Table 2, it is straightforward to admit that the ratio h/t is very small or rather that the delamination subdivides the structure in two parts: a base sublaminate whose thickness is 3.36mm and a thin sublaminate of thickness 0.64mm. In this case two analytical models can be used, the first called "thin film" (Figure 8) approximation in which the base sublaminate is assumed to be infinitely thick and the second the "thick column" in which the base sublaminate is of finite thickness but it is assumed to remain unbuckled (Chai et al., 1981).

Equivalent Young's Modulus	E_{eq}	*72GPa*
Plate Length in the load direction	L	*100mm*
Delamination length in the load direction	l	*60mm*
Thickness of plate	t	*4mm*
Thickness of the thinnest sublaminate	h	*0.64mm*
Equivalent Poisson Ratio	v	*0.3*

Table 2. Data needed for the application of the analytical model by Chai et al. (1981)

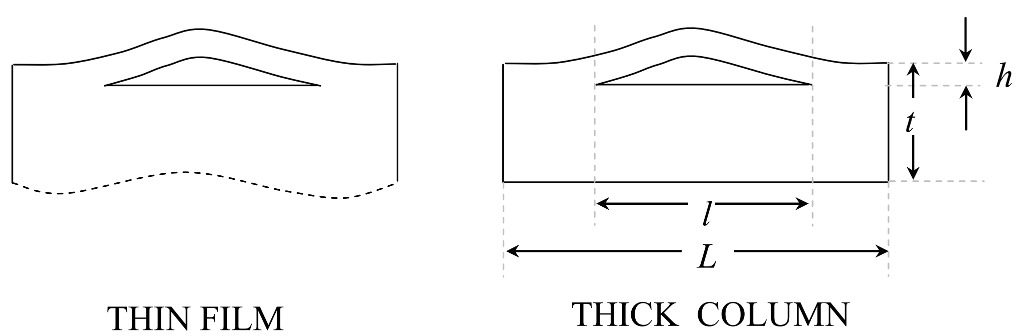

Fig. 8. Thin film and thick column delamination buckling models

The applied strain at which the delamination buckles (local buckling of the delamination) is given by the Eq. (7) (Chai et al., 1981). The expressions for the Strain Energy Release Rate at the strain ε_0 are given by Eq. (8) and Eq. (9-10) respectively for the "thin film" approximation and for the "thick column" approximation. Indeed, these analytical expressions were obtained by Chai et al., (1981) using a one dimensional modeling of the structure.

$$\varepsilon_{CR} = \frac{\pi^2}{3\left(1-\nu^2\right)}\left(\frac{h}{l}\right)^2 \tag{7}$$

$$G_a = \frac{E_{eq}h\left(1-\nu^2\right)}{2}\left(\varepsilon_0 - \varepsilon_{CR}\right)\left(\varepsilon_0 + 3\varepsilon_{CR}\right) \text{ "THIN FILM"} \tag{8}$$

$$\bar{G}_b = \frac{\pi^4 \bar{h}\left(1-\bar{h}\right)}{18k^2}\left(\bar{\varepsilon}_0 - \bar{\varepsilon}_{CR}\right)\left[\bar{\varepsilon}_0 + \bar{\varepsilon}_{CR}\left(3 + \frac{4\overline{hl}}{1-\bar{h}}\right)\right] \text{ “THICK COLUMN”} \quad (9)$$

where

$$\bar{G}_b = \frac{G_b L^4\left(1-\nu^2\right)}{Et^5};\ \bar{h} = \frac{h}{t};\ \bar{l} = \frac{l}{L};\ k = 1-\bar{h}+\overline{hl};\ \bar{\varepsilon}_{CR} = \left(\frac{\bar{h}}{\bar{l}}\right)^2;\bar{\varepsilon}_0 = \varepsilon_0\frac{3\left(1-\nu^2\right)}{\pi^2}\left(\frac{L}{t}\right)^2 \quad (10)$$

The value of the applied strain at which the Strain Energy Release Rate equals the material fracture Toughness is the ε_{GR} (applied strain at which the delamination starts growing) can be determined by manipulating Eq. (8) and Eq.(9) imposing respectively that $G_a = G_{CR}$ (Thin film) and $\varepsilon_0 = \varepsilon_{GR}$ and $G_b = G_{CR}$ when $\varepsilon_0 = \varepsilon_{GR}$. By doing so, the results in Table 3 can be obtained.

Strain necessary to cause the local buckling (if l=60mm)	ε_{CR}	*410*με
Strain necessary to cause the local buckling (if l=30mm)	ε_{CR}	*1634*με
CASE I: G_{CR}=0.2N/mm (l=60mm)		
applied strain at which the delamination starts growing “THIN FILM”	ε_{GR-a}	*2785*με
applied strain at which the delamination starts growing “THICK COLUMN”	ε_{GR-b}	*2780*με
CASE II: G_{CR}=0.2N/mm (l=30mm)		
applied strain at which the delamination starts growing “THIN FILM”	ε_{GR-a}	*2867*με
applied strain at which the delamination starts growing “THICK COLUMN”	ε_{GR-b}	*2756*με

Table 3. Analytical results obtained by using the formulae by Chai et al. (1981)

Two values for the ε_{CR} are reported in Table 3: the first is referred to the case of a length of the delamination in the direction of the applied load equal to 60mm, the second to a length of the delamination in the direction of the applied load equal to 30mm. In the benchmark selected (Sun et al., 2001), the delamination is elliptical whereas the analytical model is one-dimensional. Therefore, an intermediate value between *410*με and *1634*με should be obtained for the elliptical delamination as strain necessary to cause the local buckling.

4.2 Numerical results

Since there are only 0° and 90° plies and both the boundary conditions and the applied load are symmetric, only one quarter of the plate has been meshed by using 20 node hexahedral layered elements. For this purpose, the faces AB and AD in Figure 9 have been constrained according to symmetry conditions (ux=0 on AD and uy=0 on AB) whereas on BC and DC has been imposed uz=0. The area AEH is the debonded zone. The load is applied on BC in the x direction.

A displacement controlled non-linear analysis has been performed (Pietropaoli & Riccio, 2010c) and the results obtained are shown in Figure 10 in terms of “applied displacement” versus “out of plane displacement” graph. The value of the ε_{CR} obtained by this graph (Leissa, 1987) is above 1370με, the one computed by Sun et al. (2001) was above 1350με. Therefore, there is a good agreement between the numerical results that fall in the range individuated by using the analytical model (Table 4).

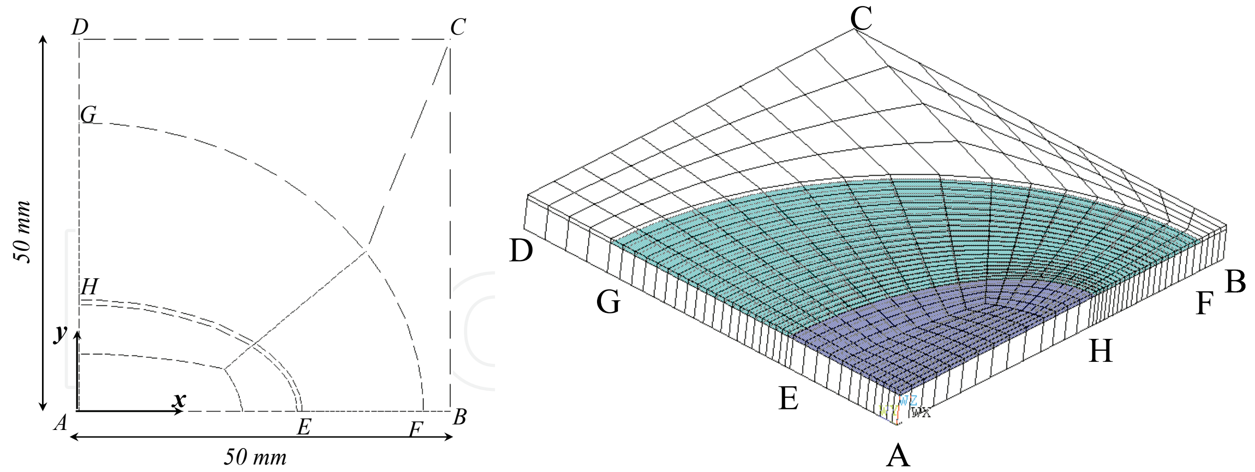

Fig. 9. Geometry and mesh of the plate with an elliptical embedded delamination

Strain necessary to cause the local buckling (analytical value)	ε_{CR}	*410-1643*με
Strain necessary to cause the local buckling (Sun et al., 2001)	ε_{CR}	*1350*με
Strain necessary to cause the local buckling determined by using Figure 7	ε_{CR}	*1370*με

Table 4. Strain necessary to cause the local buckling

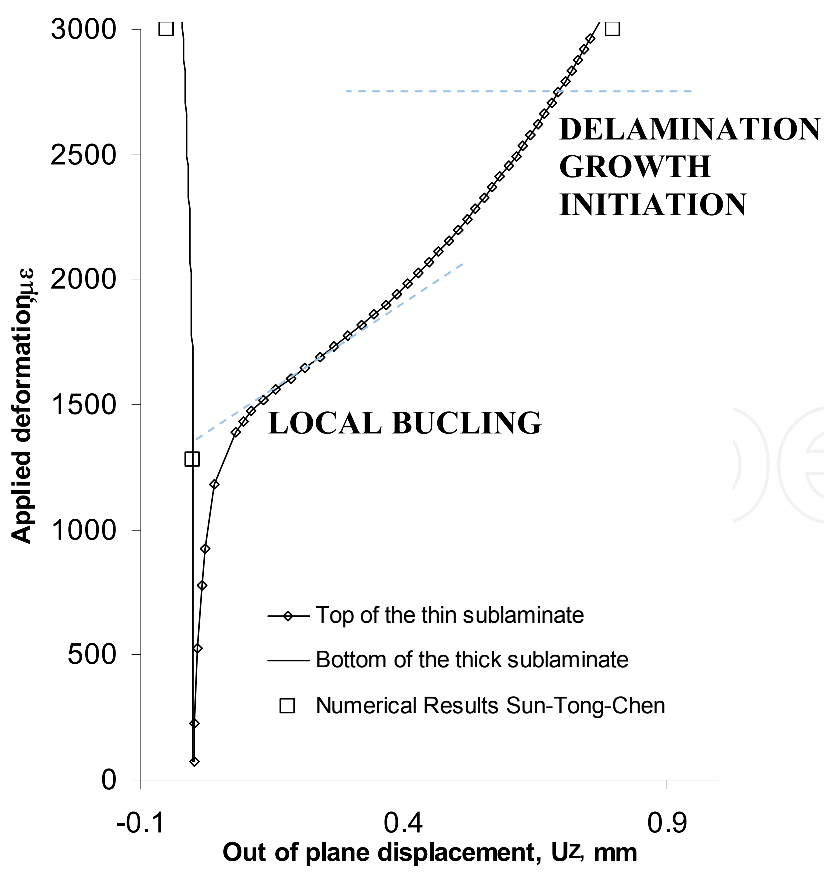

Fig. 10. Applied displacement versus out of plane displacement graph (no growth)

The Strain Energy Release Rate distributions at 2700με and 2750με obtained by using the VCCT are plotted in Figure 11 against the angle θ for the fracture modes I and II along the delamination front. The corresponding values of the failure index computed by using the power low criterion in Eq. (5) with $\alpha = 1, \beta = 1$ are shown in Figure 12.

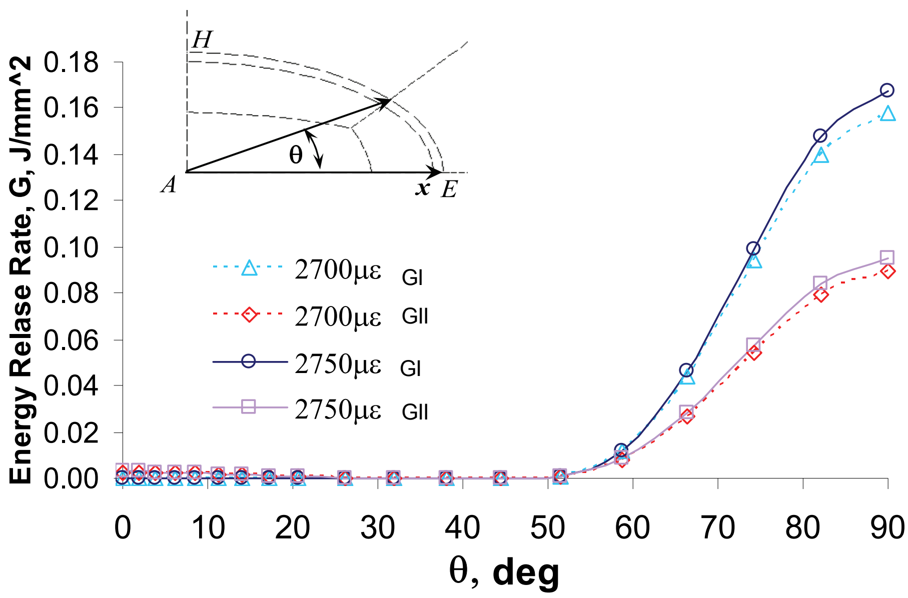

Fig. 11. Strain Energy Release Rate Distributions along the delamination front at 2700με and 2750με

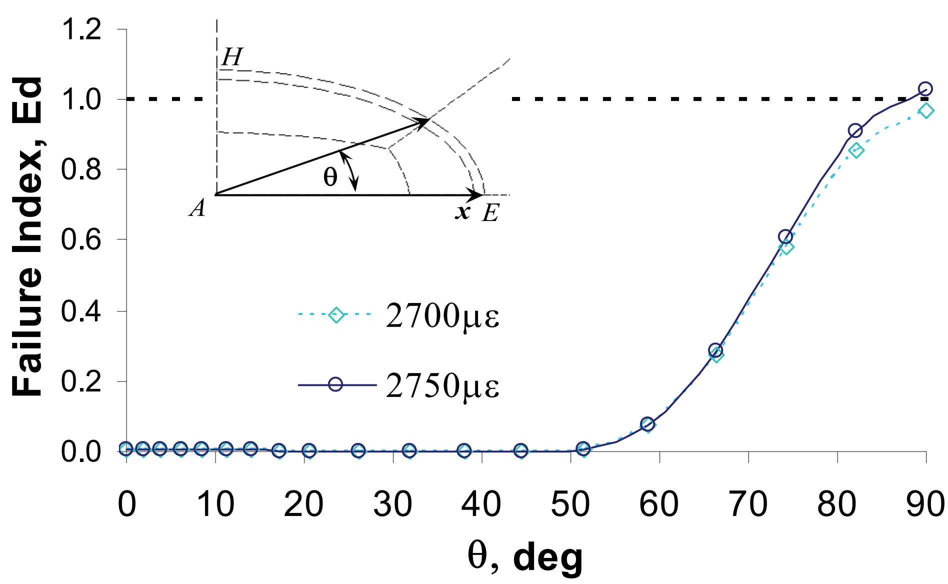

Fig. 12. Failure index distribution along the delamination front at 2700με and 2750με

The failure index becomes greater than 1 at an applied strain equal to 2750με in the range 87°<θ<90°. This means that the delamination starts growing in the direction orthogonal to the applied load and that the ε_{GR} is equal to 2750με.
In this case, two different values for the fracture toughness for the mode I and II have been considered, as reported in Table 1.

In the work by Sun et al. (2001), a Griffith type crack growth criterion was used (Eq. (4)) where the critical strain energy release rate was assumed to be equal to the one of the fracture mode I: $G_C = G_{IC}$. Furthermore, the finite element model by Sun et al., (2001) was based on the Reissner-Mindlin plate theory which neglects the transverse normal stress σ_{zz} and leads to an approximation of the shear stresses σ_{xz} and σ_{yz}. These choices have led Sun et al. (2001) to obtain an underestimated prediction of the ε_{GR} = 2000με.

applied strain at which the delamination starts growing (Sun et al., 2001)	ε_{GR}	2000με
applied strain at which the delamination starts growing (Figure 9)	ε_{GR}	2750με
applied strain at which the delamination starts growing (analytical model)	ε_{GR}	2756με-2867με

Table 5. Applied strain at which the delamination starts growing

It is straightforward to recognise in Table 5 the agreement between the numerical results obtained in this work 2750με and the range defined by the analytical model 2756με< ε_{GR} <2780με. This agreement demonstrates the effectiveness of the VCCT in predicting the delamination growth initiation.

5. Conclusion

Composites are material whose behaviour is difficult to predict by using numerical methods especially in presence of damage. However, the finite element method used in conjunction with the Virtual Crack Closure Technique (VCCT) can provide effective information in terms of global behaviour of the structure in presence of an interlaminar damage. The effectiveness of the VCCT has been proved in this Chapter through the determination the delamination growth initiation load for a composite plate with an elliptical delamination and the comparison of this value with reference results.

6. References

Abrate S. (1998), Impact on composite structures, Cambridge University Press, ISBN 9780521473897.

Altenbach, H., Altenbach, J., Kissing, W. (2004), Mechanics of Composite Structural Elements, Springer, ISBN 3540408657.

Benzeggagh, M. L., Kenane M. (1996), Measurement of Mixed-Mode Delamination Fracture Toughness of Unidirectional Glass/Epoxy Composites with Mixed-Mode Bending Apparatus. *Composites Science and Technology*, Volume 56, Issue 4, pp. 439-449,ISSN 0266-3538.

Camanho P. P., Davila C. G., De Moura M. F. (2003), Numerical simulation of Mixed-Mode Progressive Delamination in Composite Materials*, Journal of composite materials*, Volume 37, pp.1415-1438,ISSN 0021-9983.

Chai, H., Babcock, C.D.,Knauss, W. G (1981), One dimensional modelling of failure in laminated plates by delamination buckling, *International Journal of Solids and Structures*, Volume 17, pp. 1069-1083, ISSN 0020-7683.

Cook R.D. (1995), Finite Element Modeling for Stress Analysis, Wiley, ISBN 0471107743.

Davies G. A. O., Zhang X., Zhou G. and Watson S. (1994), Numerical modelling of impact damage, *Composites*, Volume 25, Issue 5, pp.342-350, ISSN 1359-835X.

Davies G. A. O., Zhang X. (1995), Impact damage prediction in carbon composite structures, *International Journal of Impact Engineering*, Volume 16, Issue 1, pp.149-170, Elsevier, ISSN 0734-743X.

Janssen M., Zuidema J. and Wanhill R.J.H. (2004), Fracture Mechanics, Spon Press Taylor & Francis, ISBN 0415346223.

Jones R. (1999), Mechanics of composite materials, Taylor and Francis, 156032712X

Kachanov L.M. (1988), Delamination buckling of composite materials, Kluwer Academic Publishers, ISBN 90247-37702.

Kardomates, G. A. (1987), Large deformation effects in the post buckling behaviour of composites with thin delaminations, *AIAA Journal*, Volume 27, pp.624-631, ISSN 0001-1452.

Klug, J., Wu, X. ,and Sun, C. T. (1996),Efficient Modeling of Postbuckling Delamination Growth in Composite Laminates Using Plate Elements, *AIAA Journal*, Volume 34, pp.178-184, ISSN 0001-1452.

Kollar L.P.,Springer G. (2007), Mechanics of composite structures, Cambridge University Press,ISBN 9780521801652.

Krueger R., O'Brien T. K. (2000), A shell/3D modeling technique for the analysis of delaminated composite laminates. NASA/TM-2000-210287.

Krueger R., (2004), The Virtual Crack Closure Technique: History, Approach and Applications, Applied Mechanics Reviews, Volume 57, Issue 2, pp.109-143, ISSN 0003-6900.

Kyoung W. M. and Kim C. G. (1995), Delamination buckling and growth of composite laminated plates with transverse shear deformation, *Journal of composite materials*, Volume 29, Issue 15, pp. 2047-2068, ISSN 0021-9983.

Leissa A. W. (1987), A Review of Laminated Composite Plate Buckling, *Applied Mechanics Reviews*, Volume 40, Issue 5, pp. 575-592, ISSN 0003-6900.

Liu Y. P., Chen C. Y., Li G. Q. (2011), A modified zigzag approach to approximate moving crack front with arbitrary shape, *Engineering Fracture Mechanics*, Volume 78, Issue 2, pp. 234-251, ISSN 0013-7944.

Mazumdar S. K. (2002), Composites manufacturing materials, product, and process engineering,CRC press, ISBN 0849305853.

Mukherjee, Y. X., Gulrajani, S. N., Mukherjee, S. and Netravali, A. N. (1994), A numerical and experimental study of delaminated layered composites, *Journal of composite materials*, Volume 28, pp.837-870, ISSN 0021-9983.

Okada H., Higashi M., Kikuchi M., Fukui Y., Kumazawa N. (2005), Three dimensional virtual crack closure-integral method (VCCM) with skewed and non-symmetric mesh arrangement at the crack front, *Engineering fracture mechanics*, Volume 72, pp.1717-1737, ISSN 0013-7944.

Orifici A. C., de Zarate Alberdi I. O., Thomson R. S., Bayandor J. (2008), Compression and post-buckling damage growth and collapse analysis of flat composite stiffened panels, *Composites Science and Technology*, Volume 68, pp. 3150–3160, ISSN 0266-3538.

Pagano N. J. and Schoeppner G. A. (2003), Delamination of polymer matrix composites: problems and assessment, Comprehensive composite materials, Elsevier Science, Volume 2, pp.433-528, ISBN: 978-0-08-042993-9.

Pagano N.J. and Pipes R.B. (1971), The influence of stacking sequence on laminate strength, *Journal of Composite materials*, volume 5, pp.50-57, ISSN 0021-9983.

Pietropaoli E., Riccio A. (2010a), A global/local finite element approach for predicting interlaminar and intralaminar damage evolution in composite stiffened panels under compressive load. *Applied Composite Materials*, DOI: DOI: 10.1007/s10443-010-9135-1, Springer, ISSN 1573-4897.

Pietropaoli E. Riccio A. (2010b), On the robustness of finite element procedures based on Virtual Crack Closure Technique and fail release approach for delamination growth phenomena. Definition and assessment of a novel methodology, *Composites Science and Technology*,Volume 70, Issue 8, pp. 1288-1300, ISSN 0266-3538.

Pietropaoli E., Riccio A. (2010c), Finite Element Analysis of the Stability (Buckling and Post-Buckling) of Composite Laminated Structures: Well Established Procedures and Challenges,*Applied Composite Materials*, DOI: 10.1007/s10443-010-9182-7, Springer, ISSN 1573-4897.

Raju I. S. (1987), Calculation of strain-energy release rates with higher order a singular finite element, *Engineering Fracture Mechanics*, Volume 28, pp. 251-274, 0013-7944.

Reeder J. R. and Crews J. H. (1990), Mixed-mode bending method for delamination testing, AIAA Journal, Vol.28,No.7, pp. 1270-1276, ISSN 0001-1452.

Reeder J. R. (2006), 3D Mixed-Mode Delamination fracture criteria-an experimental perspective, 17-20 Sep. 2006; American Society for Composites 21st Annual Technical Conference; Dearborn, MI; United States.

Riccio A., Scaramuzzino F., Perugini P. (2003), Influence of contact phenomena on embedded delaminations growth in composites, *AIAA Journal*, Volume 41, Issue 5, pp. 933-940, ISSN 0001-1452.

Riccio A., Pietropaoli E. (2008), Modeling damage propagation in composite plates with embedded delamination under compressive load, *Journal of composite materials*, Volume 42, Issue 13,pp.1309-1335, ISSN 0021-9983

Rybicki E. F., Kanninen M. F. (1997), A finite element calculation of stress intensity factors by a modified crack closure integral, *Engineering Fracture Mechanics*, Volume 9, pp. 931-938, ISSN 0013-7944.

Shen F., Lee K. H., Tay T. E. (2001), Modeling delamination growth in laminated composites, *Composites Science and Technology*, Volume 61, pp.1239-1251, , ISSN 0266-3538

Shivakumar K. N., Tan P. W., Newman J. C. Jr, (1988), A virtual crack closure technique for calculating stress intensity factors for cracked three dimensional bodies, *International Journal of Fracture*, Volume 36, R43-R50, ISSN 0376-9429.

Sun X., Tong L., and Chen H. (2001), Progressive failure analysis of laminated plates with delamination, *Journal of reinforced plastics and composites*, volume 20, pp.1370-1389, ISSN 0731-6844.

Turon A., Camanho P. P., Costa J., Dávila C. G. (2004), An Interface Damage Model for the Simulation of Delamination Under Variable-Mode Ratio in Composite Materials, NASA/TM-2004-213277

Wang J. T., Raju I. S. (1996), Strain Energy Release Rate Formulae for Skin-Stiffener Debond Modeled with Plate Elements, *Engineering Fracture Mechanics*, Volume 54, pp.211-228, ISSN 0013-7944.

Whitcomb J. D. (1989), Three-dimensional analysis of a postbuckled embedded delamination, *Journal of composite materials*, Volume 23, pp. 862-889, ISSN 0021-9983

Whitcomb J. D. (1992), Analysis of a Laminate with a Postbuckled Embedded Delamination, Including Contact Effects, *Journal of Composite Materials*. Volume 26,pp.1523-1535, ISSN 0021-9983

Xie D., Biggers S. B. (2006), Strain energy release rate calculation for a moving delamination front of arbitrary shape based on the virtual crack closure technique. Part I: Formulation and validation, *Engineering fracture mechanics,* 2006, Volume 73, Issue 6, pp.771-785, ISSN 0013-7944

Xie D., Biggers S. B. (2006). Strain energy release rate calculation for a moving delamination front of arbitrary shape based on the virtual crack closure technique. Part II: Sensitivity study on modeling details, *Engineering fracture mechanics*, Volume 73, Issue 6, pp. 786-801, ISSN 0013-7944

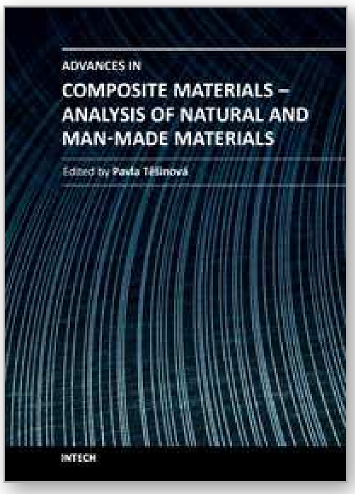

Advances in Composite Materials - Analysis of Natural and Man-Made Materials
Edited by Dr. Pavla Tesinova

ISBN 978-953-307-449-8
Hard cover, 572 pages
Publisher InTech
Published online 09, September, 2011
Published in print edition September, 2011

Composites are made up of constituent materials with high engineering potential. This potential is wide as wide is the variation of materials and structure constructions when new updates are invented every day. Technological advances in composite field are included in the equipment surrounding us daily; our lives are becoming safer, hand in hand with economical and ecological advantages. This book collects original studies concerning composite materials, their properties and testing from various points of view. Chapters are divided into groups according to their main aim. Material properties are described in innovative way either for standard components as glass, epoxy, carbon, etc. or biomaterials and natural sources materials as ramie, bone, wood, etc. Manufacturing processes are represented by moulding methods; lamination process includes monitoring during process. Innovative testing procedures are described in electrochemistry, pulse velocity, fracture toughness in macro-micro mechanical behaviour and more.